Original Article

The Interfascicular Matrix of Energy Storing Tendons Houses Heterogenous Cell Populations Disproportionately Affected by Aging

Danae E. Zamboulis[1*], Neil Marr[1], Luca Lenzi[2], Helen L. Birch[3], Hazel R. C. Screen[4], Peter D. Clegg[5], Chavaunne T. Thorpe[1]

[1]Department of Comparative Biomedical Sciences, Royal Veterinary College, London, NW1 0TU, UK.
[2]Centre for Genomic Research, University of Liverpool, Liverpool, L69 7ZB, UK.
[3]Department of Orthopaedics and Musculoskeletal Science, University College London, Royal National Orthopaedic Hospital, Stanmore, HA7 4LP, UK.
[4]Institute of Bioengineering, School of Engineering and Materials Science, Queen Mary University of London, London, E1 4NS, UK.
[5]Department of Musculoskeletal and AgingScience, Institute of Life Course and Medical Sciences, University of Liverpool, Liverpool, L7 8TX, UK.

ABSTRACT: Energy storing tendons such as the human Achilles and equine superficial digital flexor tendon (SDFT) are prone to injury, with incidence increasing with aging, peaking in the 5th decade of life in the human Achilles tendon. The interfascicular matrix (IFM), which binds tendon fascicles, plays a key role in energy storing tendon mechanics, and aging alterations to the IFM negatively impact tendon function. While the mechanical role of the IFM in tendon function is well-established, the biological role of IFM-resident cell populations remains to be elucidated. Therefore, the aim of this study was to identify IFM-resident cell populations and establish how these populations are affected by aging. Cells from young and old SDFTs were subjected to single cell RNA-sequencing, and immunolabelling for markers of each resulting population used to localise cell clusters. Eleven cell clusters were identified, including tenocytes, endothelial cells, mural cells, and immune cells. One tenocyte cluster localised to the fascicular matrix, whereas nine clusters localised to the IFM. Interfascicular tenocytes and mural cells were preferentially affected by aging, with differential expression of genes related to senescence, dysregulated proteostasis and inflammation. This is the first study to establish heterogeneity in IFM cell populations, and to identify age-related alterations specific to IFM-localised cells.

Key words: interfascicular matrix, tendon aging, single cell sequencing, tendon cell populations, proteostasis, senescence

INTRODUCTION

Tendons transmit muscle-generated force to the skeleton, and specific tendons also play a key role in locomotory efficiency by storing and returning energy with each stride. These energy storing tendons are prone to age-related degeneration and subsequent injury [1, 2], however the causes of this degeneration remain to be established. The human Achilles tendon and equine superficial digital flexor tendon (SDFT) are the predominant energy storing tendons in the human and horse respectively [3, 4]. Indeed, the equine SDFT is a relevant and well-established model in which to study tendon aging, due to similarities in structure and function

*Correspondence should be addressed to: Dr. Danae E. Zamboulis, [1]Department of Comparative Biomedical Sciences, Royal Veterinary College, London, NW1 0TU, UK. Email: dzamboulis@rvc.ac.uk.

with the human Achilles, as well as shared epidemiology and aetiology of disease, and poor healing after injury [5, 6].

Tendons are rich in extracellular matrix proteins, predominantly collagen type I, which is arranged in a hierarchical manner and interspersed with non-collagenous proteins [7]. At the largest level of the hierarchy, tendon fascicles are bound by the interfascicular matrix (IFM), a looser connective tissue matrix rich in proteoglycans, minor collagens, and elastin [8-11]. Cells, collectively referred to as tenocytes, are found in both the fascicles and IFM regions, with greater cell density within the IFM [8]. There is also evidence of other cell populations present within tendon, with single-cell RNA sequencing (scRNAseq) of murine and human tendon revealing several tenocyte populations, as well as endothelial, mural and immune cell populations [12, 13]. However, the tendons used in these studies generally have limited energy storing capacity and a less prominent IFM, therefore it has not yet been established which cell populations localise to the IFM, nor how tendon cell populations may be differentially affected by aging.

The IFM plays a key role in the function of energy storing tendons by allowing sliding and recoil between fascicles, carrying the load between discontinuous tendon subcomponents [14], providing the whole tendon with high strain capacity and fatigue resistance [15-17] and contributing to the tendon's viscoelastic response to dynamic loading and long-term stress relaxation [18]. The IFM is disproportionately affected by aging, with IFM stiffening, reduced fatigue resistance and impaired recoverability reported, all associated with an increased risk of injury in aging tendon [19-21]. Therefore, characterising the role of IFM cell populations in maintaining tendon homeostasis, and establishing how IFM cell populations are impacted by aging is crucial to elucidate the drivers of age-related alterations in tendon structure-function relationships and how these lead to increased risk of injury with aging. Therefore, the aim of this study was to use single-cell RNA sequencing, combined with immunolabelling, to identify and localise IFM-resident cell populations in the equine SDFT and establish how these populations are affected by aging.

MATERIALS AND METHODS

Sample acquisition and preparation

Forelimbs, distal to the carpus, were collected from young (n=4; age range:3-4 years) and aged (n=4; age: >17 years) horses euthanised for reasons unrelated to this project from a commercial abattoir. Sample collection was approved by the Royal Veterinary College's Clinical Research Ethical Review Board (URN 2016 1627B). Two

~3 cm pieces of superficial digital flexor tendon (SDFT) were harvested from the mid-metacarpal region of one forelimb from each horse on the same day as euthanasia. One piece was snap frozen in isopentane in liquid nitrogen for subsequent histology and spatial analysis of cell niches, and the other was digested to obtain cell populations as described below.

Tendon digestion and generation of single cell suspensions

SDFT pieces were washed several times in Dulbecco's Modified Eagle's Medium (DMEM) with antibiotics and antimycotics, the epitenon was removed, and the tendon core was finely minced (a few mm^3) under sterile conditions. Samples were digested (3 mg/mL collagenase type 2, 1 mg/mL dispase, 100 μg/mL DNase I in DMEM supplemented with 50 U/mL penicillin, 50 μg/mL streptomycin, 0.5 μg/mL amphotericin B and 10 % foetal bovine serum) for 4 h at 37° C with agitation. Samples were strained (40 μm filters) and dead cells removed using a dead cell removal kit according to the manufacturer's instructions (Miltenyi Biotec). Cell viability was determined using trypan blue staining and cells were counted using a haemocytometer, followed by resuspension in 0.4 % BSA in PBS at ~1000 cells/μl. Viability was ≥ 90 % for all samples.

Single cell RNA sequencing

Approximately 6,500 cells from each sample were prepared for scRNAseq using a Chromium single cell 3' reagent kit (10x Genomics) according to the manufacturer's instructions. Libraries were pooled and sequenced on an Illumina® NovaSeq 6000 (Illumina®, San Diego, USA) on an SP flow cell, generating 28 bp x 91 bp paired-end reads. Data have been deposited at EMBL-EBI under the project ID PRJEB57256.

Bioinformatic Analysis

Reads were aligned using Cell Ranger (v.6.0.0) on horse genome (EquCab3.0.103). Barcode swapping events and empty droplets were excluded using DropletUtils [22] and subsequent downstream analysis was performed using Seurat (v4.1.1) in R Studio (v2021.09.2) [23]. Quality control was performed as follows: filters: >500 unique molecular identifiers/cell; 250-5500 genes/cell; Log10Gene Per UMI >0.8; <10% mitochondrial reads/cell. Any genes expressed in less than 10 cells were excluded from subsequent analysis. Following data normalization by SCTransform [24], principal component analysis and integration was performed using Harmony [25]. The 'FindCluster' function was used to identify cell

clusters (0.2 resolution). Post-clustering, further manual quality control revealed the presence of one cluster comprised of cells originating predominantly from one sample. Further analysis of this cluster indicated it likely consisted of cells derived from the epitenon and therefore it was excluded from any further analysis. Genes differentially expressed (DE) between remaining clusters were identified using the 'FindAllMarkers' function in Seurat with the default Wilcoxon Rank Sum test and a log2 fold change (log2FC) threshold of 0.25 and adjusted p value 0.05 (adjusted p-value based on Bonferroni correction using all the features in the dataset).

Analysis of age-related alterations

Genes differentially expressed (DE) between age groups within each cluster were identified using the 'FindAllMarkers' function in Seurat using the default Wilcoxon Rank Sum test and a log2FC threshold of 0.25 and adjusted p-value 0.05 (adjusted p-value based on Bonferroni correction using all the features in the dataset). Of these DE genes, those associated with aging were identified and classified using the Aging Atlas [26]. The top 25 genes in each cluster were compared between young and old to identify the number of genes conserved with aging. To assess changes in inflammatory gene signatures, DE genes with aging associated with the GOTerm 'inflammatory response' (GO:0006954) [27] were identified.

Analysis of tenocyte clusters

The tenocyte clusters IFM, FM, and MixT, were re-clustered (0.1 resolution) and genes DE between subclusters and with aging identified as described above (Wilcoxon Rank Sum test and a log2FC threshold of 0.25 and adjusted p value 0.05). The top 50 DE matrisome-associated genes between subclusters were identified and classified according to matrisome categories [28], and DE matrisome-associated genes with aging were identified. Heatmaps with circular layout were created using the R package "circlize" [29].

Cell differentiation state analysis

Cell differentiation state analysis was carried out with the open source package CytoTRACE (Cellular (Cyto) Trajectory Reconstruction Analysis using gene Counts and Expression) [30]; a computational method that predicts the differentiation state of cells from single-cell RNA-sequencing data based on the number of detectably expressed genes per cell, or gene counts which are determinants of developmental potential. The differentiation state of tenocytes was visualised on UMAPs of young and old re-clustered tenocytes and raincloud plots [31], ranking the order of differentiation state for young re-clustered tenocytes.

Cell communication analysis

Cell-to-cell communication analysis was performed using the open source R package CellChat [32] focusing on secreted signalling interactions also termed paracrine/ autocrine signalling interactions. To infer the cell cluster-specific communications, CellChat identified over-expressed ligand-receptor interactions by identifying over-expressed ligands or receptors in cell clusters. To quantify communications between two groups, CellChat associates each interaction with a probability value and significant interactions are identified using a permutation test (p<0.05). CellChat was therefore used to compare cell-cell communication between young and old samples to identify interactions between cell clusters that were significantly changed with aging, alongside identifying how signalling sources and targets changed. In addition, CellChat identified significantly decreased or increased signalling pathways in aging by comparing the information flow for each signalling pathway; the information flow is defined by the sum of communication probability among all pairs of cell groups in the inferred network. Finally, outgoing and incoming signalling pathways were visualised for young and old samples to identify age-related differences in pathways for each cell cluster. Heatmaps were used to illustrate the cluster communications and pathways along with their differences with aging.

Statistical analysis

Additional statistical analysis was carried out for the comparison of cell percentages per cluster between young and aged tendons and cell percentages per cycling phase and cluster between young and aged tendons. Normality of the data was assessed using a Shapiro-Wilk test (p < 0.05). Normally distributed datasets were analysed with an unpaired t-test (p < 0.05), using a Welch's correction when unequal variance was noted, and non-normally distributed datasets were analysed with a Mann-Whitney test (p < 0.05) (Prism v9.0.0).

Spatial distribution

Longitudinal cryosections were cut from the snap-frozen SDFT samples at a thickness of 20 μm and adhered to glass slides. Haematoxylin and eosin staining was performed using standard protocols to ensure that all samples displayed a normal morphology and were free from any microscopic signs of injury.

Immunohistochemistry was performed as described previously to localise markers for each cell cluster; details of primary and secondary antibodies, and blocking conditions are shown in Table S1 [33]. Briefly, tendon sections were thawed, fixed in ice cold acetone:methanol (50:50) for 5 minutes, washed with tris-buffered saline (TBS), blocked and then incubated in primary antibody overnight at 4° C. Following TBS washes and hydrogen peroxide treatment (0.3 %, 15 min), secondary antibodies were applied at room temperature for 1 hour. Staining was developed with 3,3'-diaminobenzidine (5 min, Vector Labs, San Francisco, CA, USA), and sections were counterstained with haematoxylin for 30 s, dehydrated (Gemini AS Automated Slide Stainer, Thermo Scientific) and mounted with DPX. Sections were cured overnight and imaged using brightfield microscopy (DM4000B upright microscope; objectives: 10× HC PL FLUOTAR PH1, 20× HC PL FLUOTAR PH2; DFC550 colour camera; LAS-X version 3.7 software (Leica Microsystems)). Negative controls were carried out with the omission of primary antibody (Supplementary Fig. 3).
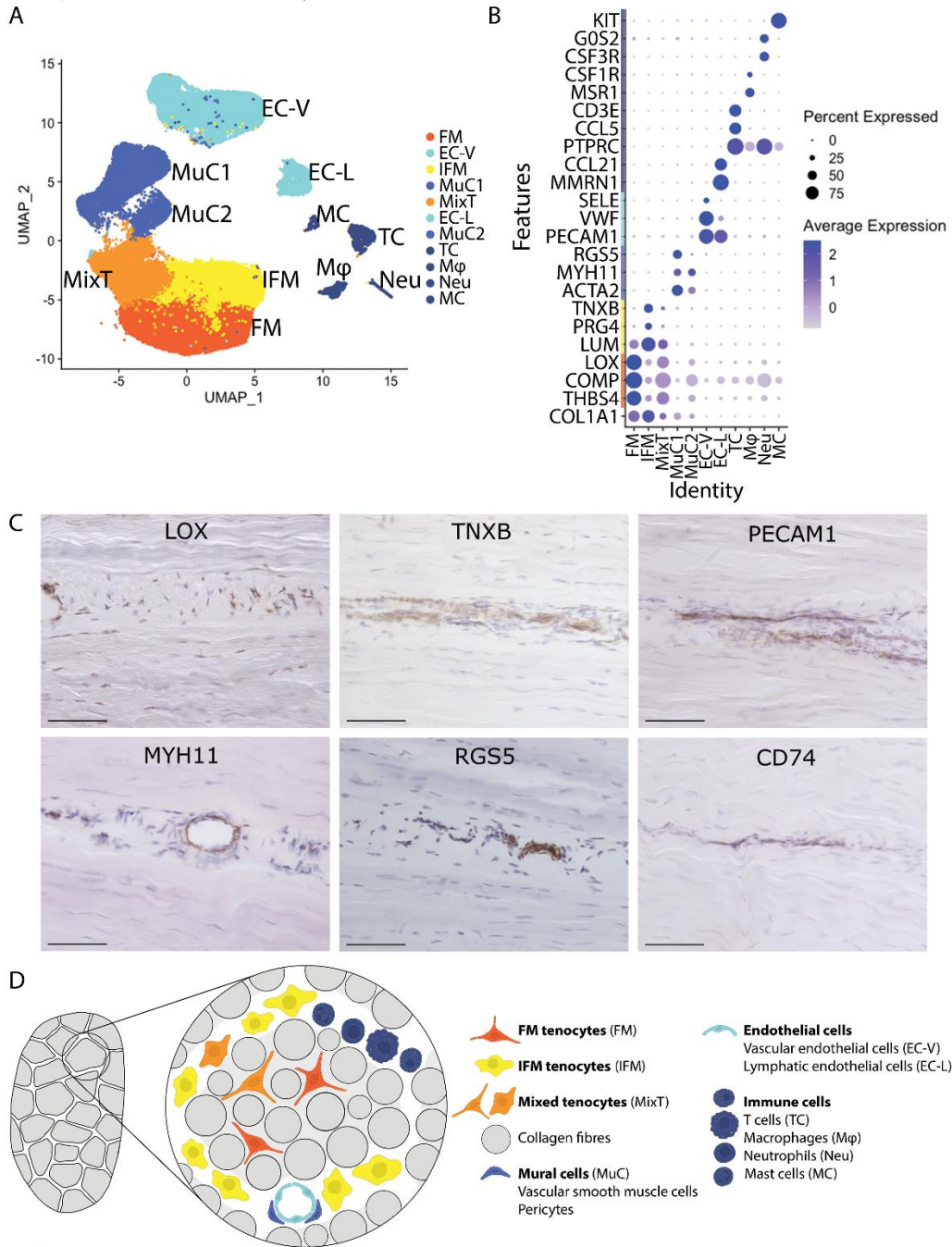
Figure 1. 11 cell clusters are present in equine tendon. (A) Uniform Manifold Approximation and Projection (UMAP) dimensionality reduction demonstrates the presence of 11 clusters, based on differential gene expression, namely FM tenocytes "FM", IFM tenocytes "IFM", mixed tenocytes "MixT", mural cells "MuC1" and "MuC2", vascular endothelial cells "EC-V", lymphatic endothelial cells "EC-L", T cells "TC", macrophages "Mφ", neutrophils "Neu", and mast cells "MC". Each cluster consists of cells originating from young and old donors (n=4/age group). (B) Dot plot showing genes used to differentiate and identify the clusters. Scale indicates average expression and ranges from grey = 0 to blue = 2, dot size indicates the percentage of cells expressing the gene. (C) Immunolabelling of longitudinal tendon sections reveal that all cells within fascicles, and some within the IFM compartment are positive for LOX, and cells within the IFM compartment show presence of TNXB, the endothelial cell marker PECAM1 validating the presence of both endothelial clusters EC-V and EC-L, the mural cell markers MYH11 and RGS5 for both mural cell clusters MuC1 and MuC2, and the immune cell marker CD74 for all immune cell clusters, TC, Mφ, Neu, MC (negative control in Figure S3). Scale bar 75 µm. (D) Schematic of tendon demonstrating location of the different cell populations identified.

RESULTS

11 cell clusters are present in equine tendon

To characterise young and aged tendon populations in an energy storing tendon, scRNA-seq was performed on SDFT cells isolated from 4 young and 4 old horses (Supplementary Fig. 1). Following quality control and filtering, data were derived from a total of 59273 cells which clustered into 11 distinct clusters (Fig. 1A). Three tenocyte clusters were identified based on expressions of *COL1A1*, *COL3A1*, *COMP, DCN, LUM* and *LOX*. The largest of these clusters was defined as FM tenocytes (FM), based on higher levels of expression of *COMP*, *LOX* and *THBS4* (Fig. 1B), which are localised to the fascicular matrix [34, 35]. The second tenocyte cluster was defined as IFM tenocytes (IFM) due to their differential expression of *PRG4*, a well-established marker of IFM cells [9, 36], and *TNXB* (Fig. 1B), localisation of which was confirmed using immunolabelling (Fig. 1C). The third tenocyte cluster expressed markers found in both IFM and FM tenocyte clusters (*COMP*, *LOX*, *THBS4, TNXB, LUM, PRG4)* and is referred to as mixed tenocytes (MixT). Clustering of tenocytes in the "MixT" cluster was driven by significantly lower expression of ribosome biogenesis-specific genes (Supplementary Fig. 2A), which was more pronounced in aged tendons. Two mural cell clusters (MuC1&2) were identified which localised to the IFM region, based on differential expression of the vascular smooth muscle and pericyte markers *RGS5*, *MYH11* and *ACTA2* [37, 38] (Fig. 1B). Immunolabelling for these markers revealed the mural cells surrounded vessels in the IFM and were absent in the fascicles (Fig. 1C). Similar to the MixT cluster, clustering of mural cells in the MuC2 cluster was driven by lower expression of ribosomal biogenesis genes (Supplementary Fig. 2B). Vascular endothelial cells, (EC_V) expressing *PECAM1*, *VWF* and *SELE*, and lymphatic endothelial cells (EC_L), expressing *PECAM1*, *MMRN1* and *CCL21* also localised to the IFM region (Fig. 1B and C). Four immune cell clusters were

identified, based on expression of *PTPRC* and *CD74*, which localised to the IFM (Fig. 1B and C). These clusters were further identified as T cells (TC; *CCL5* and *CD3E*), macrophages (Mφ; *CSF1R* and *G0S2*), neutrophils (Neu; *MSR1* and *CSF1R*) and mast cells (MC; *KIT*) (Fig. 1B).

IFM tenocytes and mural cells are preferentially affected by aging

To establish the effect of aging on tendon cell populations, the size of each cluster and the number of differentially expressed (DE) genes in each cell cluster from young and old tendons was assessed. The number of cells in MuC2, as a proportion of total cell number, increased significantly with aging, whereas the number of Mφ, as a proportion of total cell number, decreased with aging (Fig. 2A). Many genes within each cluster were also DE with aging (Fig. 2B). Clusters IFM and MuC2 were disproportionately affected by aging, with 466 and 902 DE genes respectively. The Aging Atlas [26] was used to identify DE genes in each cluster associated with aging-related dysfunction. Many of the DE aging genes were associated with senescence and senescence-associated secretory phenotype, as well as loss of proteostasis (Fig. 2C), particularly in IFM and MuC2 clusters (Fig. 2D). Further, comparison of the top 25 markers of each cluster (most highly expressed cluster differentiating genes) between young and old samples revealed age-dependent loss of the top genes characterising each cluster for the IFM, MixT and MuC2 clusters (Fig. 2E). Many genes associated with inflammation (GOTerm: inflammatory response, GO:0006954) [27] were also DE with aging, particularly in IFM and MuC2 clusters (Fig. 2F). Aging also had an effect on cell cycling for the IFM tenocyte and the MuC1 clusters only, where there was a significantly larger percentage of cells classifying in S phase in old samples compared to young samples in the IFM tenocyte cluster and the opposite for the MuC1 cluster (Supplementary Fig. 4).
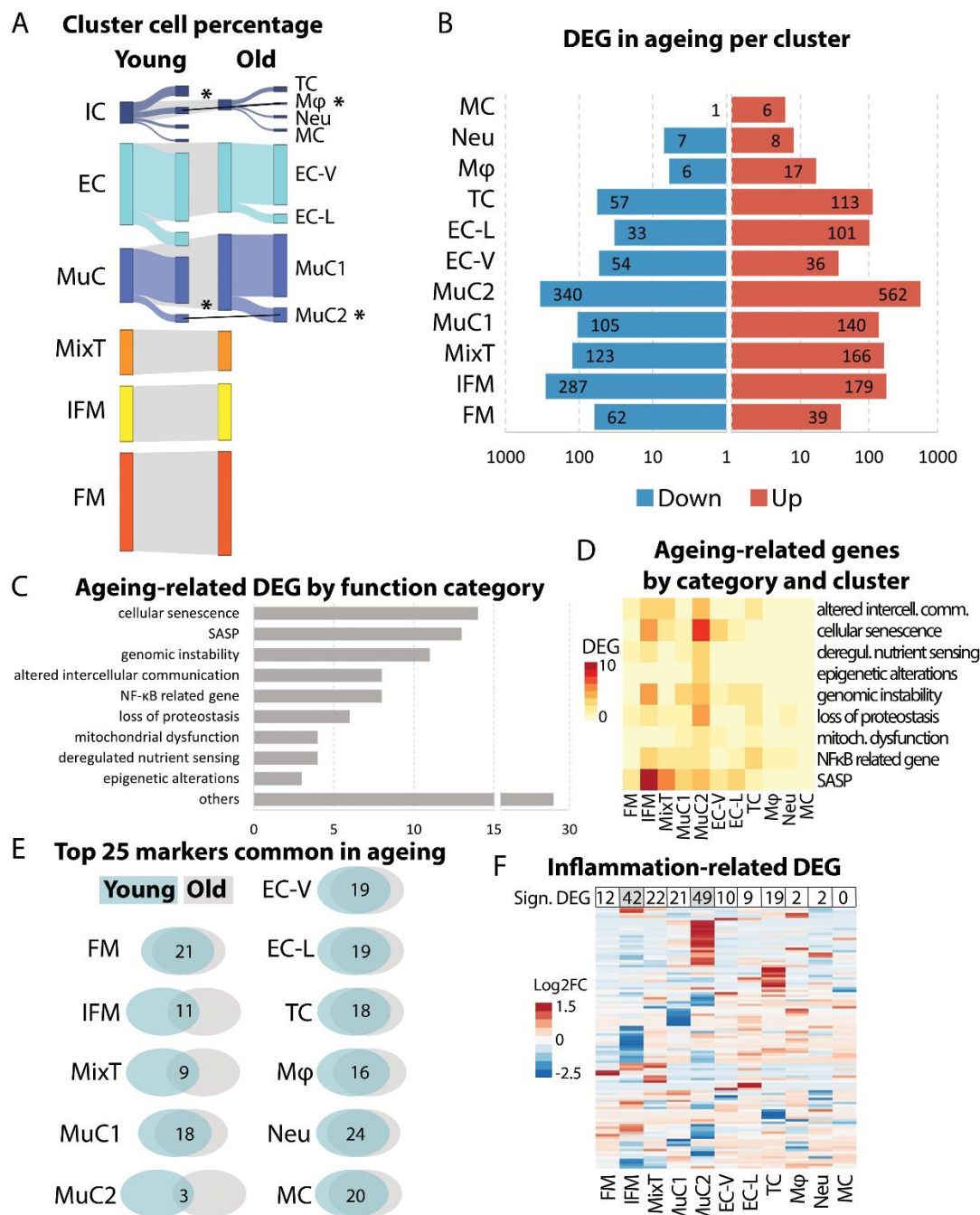
Figure 2. IFM tenocytes and mural cells are preferentially affected by aging (n=4/age group). (A) The percentage of cells in the majority of clusters was predominantly unaffected by aging, except for an increase in the proportion of cells in mural cell cluster 2 (MuC2; p=0.049, unpaired t-test) and a decrease in the proportion of macrophages (Mφ; p=0.039, unpaired t-test). Significance is indicated by*. **(B)** The number of differentially expressed genes (DEGs) with aging varied between clusters, with the highest number of DEGs in MuC2 and IFM clusters (Wilcoxon Rank Sum test, log2FC threshold 0.25, adj. p < 0.05). Data are plotted on a $\log_{10}$ scale. **(C)** Aging-related DEGs (Aging Atlas [26]) between young and old tendon cells were primarily associated with senescence and the senescence-associated secretory pathway (SASP). **(D)** Heatmap demonstrating IFM tenocyte and MuC2 clusters had the greatest number of aging related DEGs and in particular DEGs associated with senescence and SASP. Scale indicates number of genes and ranges from yellow = 0, to red = 10. **(E)** Venn diagrams showing the number of top 25 markers in each cluster that are maintained with aging. An age-dependent loss of the top genes characterising each cluster is observed for the IFM tenocyte, MixT and MuC2 clusters. **(F)** Heatmap showing IFM tenocyte and MuC2 clusters had most DE inflammation-related genes (GOTerm: inflammatory response, GO:0006954) with aging. Scale indicates log2FC and ranges from blue = –2.5, to white = 0, to red = 1.5.
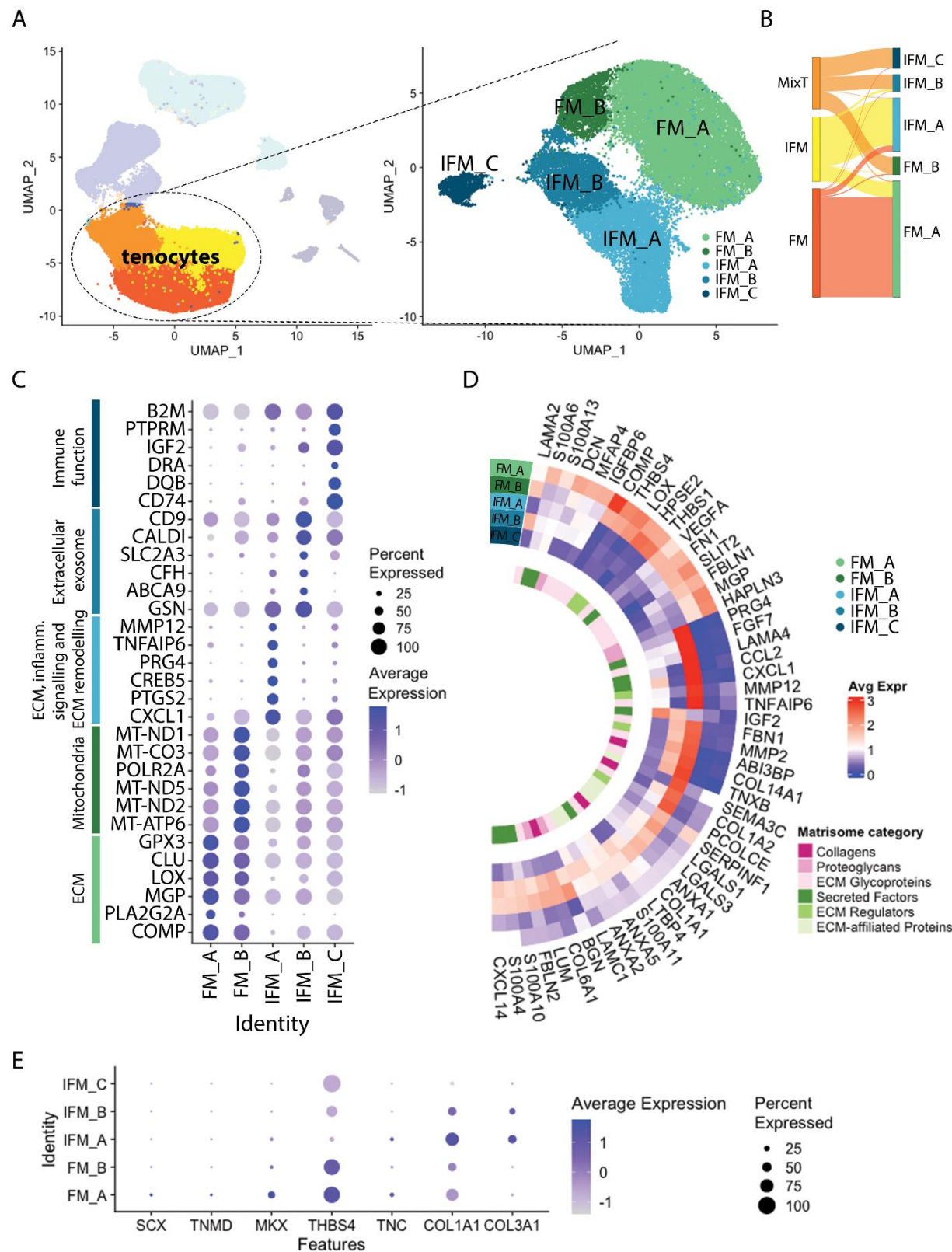
Figure 3. Sub-clustering reveals the presence of 5 tenocyte subclusters (n=4/age group). (A) Tenocyte subclusters were identified as FM_A, FM_B, IFM_A, IFM_B, and IFM_C, based on their marker expression. **(B)** Sankey diagram showing the provenance of each subcluster cell in relation to the original clusters. **(C)** Dot plot showing the top 5 differentially expressed markers and associated functions in each subcluster (Wilcoxon Rank Sum test, log2FC threshold 0.25, adj. p < 0.05). Scale

indicates average expression and ranges from grey = -1 to blue = >1, dot size indicates the percentage of cells expressing the gene. **(D)** Heatmap showing average expression of the top 50 DE matrisomal genes across tenocyte subclusters in each tenocyte subcluster, with matrisome category indicated (Wilcoxon Rank Sum test, log2FC threshold 0.25, adj. p < 0.05). Scale indicates average expression and ranges from blue = 0, to white = 1, to red = 3. **(E)** Dot plot of established tenocyte lineage genes and their expression across the tenocytes subclusters. *MKX* and *THBS4* are predominantly expressed in FM subclusters whilst *COL1A1* and *COL3A1* in IFM subclusters. Scale indicates average expression and ranges from grey = -1 to blue = >1, dot size indicates the percentage of cells expressing the gene.

Sub-clustering reveals the presence of 5 tenocyte subclusters

Re-clustering of tenocyte populations alone identified 5 subclusters (Fig. 3A), 3 of which localised to the IFM, "IFM_A", "IFM_B", and "IFM_C", and 2 that were found in the fascicular matrix, "FM_A" and "FM_B", based on the initial IFM or FM identity of re-clustered cells (Fig. 3B) and on marker similarity with either the IFM or FM cluster, including DE of ECM genes *COMP, LOX, PRG4, TNXB*, *COL14A1*, *FAP* (Supplementary Fig. 5). Subclusters IFM_A and FM_A mainly comprised of cells from the original IFM cluster and FM cluster, respectively, whilst subclusters IFM_B, IFM_C, and FM_B mainly comprised of cells originating from the MixT cluster (Fig. 3B). The top markers of each subcluster (most highly expressed markers) revealed markers for the FM_A subcluster were mainly associated with ECM production whereas FM_B top markers showed a high number of mitochondria-related genes. Further analysis of cluster FM_B, omitting the mitochondria-related genes in case they were masking other less expressed genes with significant functions, revealed markers of FM_B cluster were associated with response to stress. Markers for the IFM_A cluster showed gene expression related to the ECM, signalling in inflammation, and ECM remodelling. IFM_B top markers were associated with extracellular exosomes and IFM_C showed higher expression of genes related to immune function (Fig. 3C).

Analysis of matrisomal genes in young tenocyte clusters revealed distinct matrisome expression patterns between FM and IFM clusters, with clusters FM_A and IFM_A having the highest matrisome gene expression and IFM_C having the lowest matrisome gene expression (Fig. 3D). FM clusters had the highest expression of *DCN*, glycoproteins *COMP*, *THBS1*, and *THBS4*, and ECM-related genes *LOX* (cross-linking) and *HPSE2* (matrix remodelling). IFM clusters had the highest expression of collagens such as *COL1A2*, *COL14A1* (exclusive to the IFM) and *COL6A1* as well as proteoglycans *BGN* and *PRG4* and glycoproteins *TNXB* and *FBN1*. IFM clusters also showed higher gene expression of calcium binding proteins *S100A11*, *S100A4*, and *S100A10* which are involved in cell cycle progression and differentiation as well as cell motility and, when secreted, stimulation of cytokine production [39, 40]. Cluster IFM_C had the

lowest matrisome expression but highly expressed secreted factors *IGF2* and *CXCL1*. Interestingly, FM and IFM subclusters had differential expressions of laminin subunits with *LAMA2* expressed by FM subclusters (mostly FM_B) and IFM_B whilst *LAMA4* and *LAMC1* were expressed by IFM subclusters (mainly IFM_A and IFM_B, respectively). Similarly, fibulin expression revealed compartment-specific expression with *FBLN1* mostly expressed in FM clusters and *FBLN2* in IFM subclusters.

Expression of classical tenocyte lineage genes revealed *MKX* and *THBS4* expression in both FM subclusters and *COL1A1* and *COL3A1* expression in IFM_A and IFM_B clusters. *SCX* and *TNMD* only showed trace expression in FM_A subcluster (Fig. 3E). The more recently identified tenocyte marker IGFBP6 [41] also showed predominant expression in the FM_A subcluster, with lower expression in subclusters IFM_A and IFM_B.
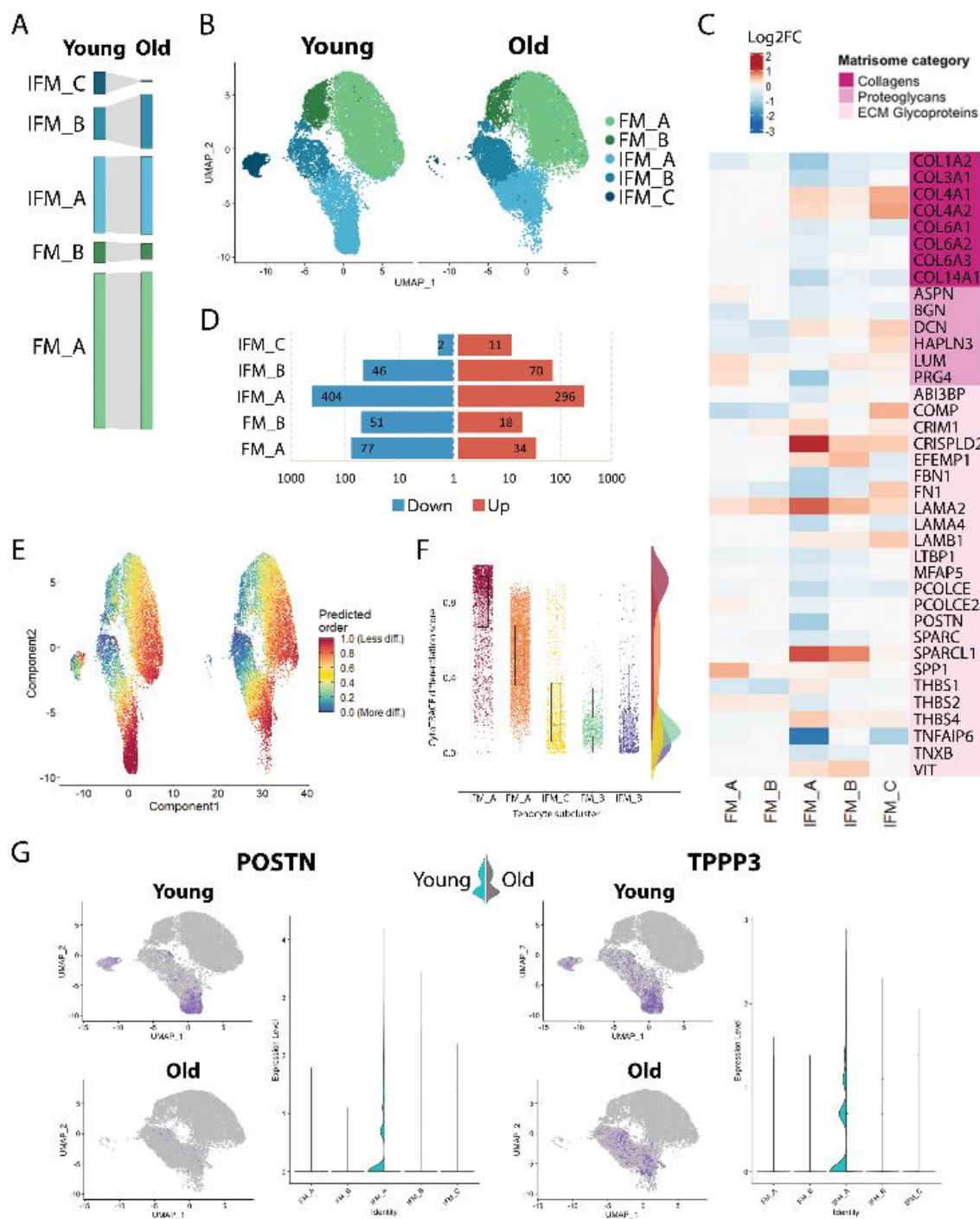
Tenocyte aging is predominantly observed in IFM subclusters

There were no significant changes in the proportional size of tenocyte subclusters with aging despite the apparent decrease in IFM_C subcluster size in old samples and concurrent increase in IFM_B subcluster size, as a percentage of total cells (Fig. 4A). IFM_A subcluster appeared to change shape without any significant size change. An elongated tip at the bottom of the IFM_A cluster (Fig. 4B) with presence of less differentiated cells (predicted, CytoTRACE) (Fig. 4E and F) and expression of *POSTN* and *TPPP3* (Fig. 4G) which have been associated with a progenitor phenotype in tendon cells [42, 43] is observed in young samples whilst absent from old samples (Fig. 4B,E-G). Concurrently, expression of *POSTN* and *TPPP3* identified/localised to the IFM_A cluster was significantly decreased with aging (Fig. 4G). IFM subclusters also showed the most DE genes with aging, particularly subcluster IFM_A (Fig. 4C), with DE genes related to the ECM, signalling in inflammation, and ECM remodelling. Subcluster IFM_A also had the most significantly DE core matrisome genes (Fig. 4D). Differential expression of core matrisome genes further highlighted a decrease in collagen gene expression in aged tenocytes (*COL1A1*, *COL3A1*, *COL6A1-3*, *COL14A1*) with the exception of *COL4A1-2*, which increased in the

IFM subclusters specifically. Other genes encoding important components of the tendon ECM, such as proteoglycans *ASPN*, *BGN* and *PRG4* and glycoprotein *TNXB*, were generally downregulated in aged tenocytes. *FBN1* and *MFAP5,* which are associated with the elastic properties of tendons, were also downregulated in all tenocyte clusters with aging whilst *SPP1* (encoding osteopontin) which is involved in tendon matrix remodelling [44] was upregulated. Interestingly, genes encoding proteins with an important role in fascicular matrix composition such as glycoproteins *COMP* and *THBS4*, proteoglycan *DCN* and cross-linking *LOX*, appeared to decrease in the FM subclusters and increase in the IFM subclusters (Fig. 4D and Supplementary Fig. 6). Finally, *LAMA2* expression increased in all tenocyte subclusters whilst *LAMA4* decreased in all subclusters.

Figure 4. Tenocyte aging is predominantly observed in IFM subclusters (n=4/age group). (A) The percentage of cells in the subclusters was not statistically significantly affected by aging, despite an apparent decrease in IFM_C cell number. **(B)** UMAP of tenocyte subclusters in young and old tendons; the distribution of cells in subcluster IFM_A changes with aging. **(C)** The number of DEGs with aging varied between subclusters, with the highest number of DEGs in the IFM_A clusters (Wilcoxon Rank Sum test, log2FC threshold 0.25, adj. $p < 0.05$). Data are plotted on a $\log_{10}$ scale. **(D)** Heatmap showing DE of selected core matrisome genes with aging in each tenocyte subcluster (Wilcoxon Rank Sum test, log2FC threshold 0.25, adj. $p < 0.05$). Scale indicates log2FC and ranges from blue = –3, to white = 0, to red = 2. **(E)** UMAP of tenocyte subclusters with prediction of differentiation state in the young and old tenocytes and **(F)** raincloud plot of tenocyte subclusters in young samples by order of least differentiation (CytoTRACE). Subcluster IFM_A has the largest number of least differentiated cells in young samples (raincloud plot and UMAP), which are located particularly in the elongated tip at the bottom of the subcluster. Whereas in old samples, this elongated tip of the IFM_A subcluster is absent and a reduction in the number of least differentiated cells is noted. Scale ranges from blue = more differentiated to red = least differentiated through green, yellow and orange. **(G)** UMAP and violin split plot of *POSTN* and *TPPP3* expression in tenocyte subclusters in young and old tendons. *POSTN* and *TPPP3* expression, which has been associated with a progenitor phenotype in tendon cells, is observed in young samples in the elongated tip at the bottom of subcluster IFM_A and it is significantly decreased with aging. Color indicates expression and ranges from grey = 0 to blue = 3.

FM and IFM tenocyte clusters become the primary sources of outgoing signalling in aging

To examine the cell communication between different cell types, we performed cell-to-cell communication analysis using "CellChat", a package that uses manually curated literature-supported ligand-receptor interactions [32]. Here, we focused on "secreted signalling" interactions in order to avoid overcrowding due to the abundance of ECM-cell interactions and cell-cell interactions. We unveiled 230 secreted signalling interactions in young tendon cells and 238 secreted signalling interactions in old tendon cells (interaction strength 1.939 and 2.326 respectively). Mural cells (MuC1), followed by the tenocytes (FM, IFM), predominated in outgoing signalling in young tendon, whilst incoming signals were mainly received by vascular endothelial cells (EC-V) followed by macrophages (Mφ) and T cells (TC) both in young and old tendon (Fig. 5A). With aging, the FM and IFM tenocyte clusters showed the largest change in outgoing secreted signalling, increasing their signalling interaction strength and becoming the primary sources of outgoing signalling in old tendon cells. More specifically, the FM and IFM tenocytes clusters increased their signalling interaction strength to all clusters apart from the mixed tenocyte cluster (MixT), with signals to the mural cells (MuC2) and T cells (TC) showing the biggest increase. These clusters, MuC2, TC and MixT, were also the target clusters that showed the most changes in incoming secreted signalling with aging, with the MuC2 and TC clusters showing increased incoming signalling interaction strength with aging and the MixT cluster decreased interaction strength (Fig. 5A). Pathways such as non-canonical WNT were downregulated with aging whilst others such as the growth factor pathways VEGF, IGF, EGF, FGF were upregulated in old tendon (Fig. 5B). In particular, FM tenocytes in young tendons exerted a strong signal in

Visfatin, ncWNT, and EGF signalling, IFM tenocytes in FGF, SEMA3, and ncWNT signalling, and MixT cells in MIF signalling (Fig. 5C). On the other hand, FM tenocytes in young tendons received a strong signal from ncWNT signalling and IFM tenocytes from TGFb and EGF signalling. Tenocyte-related enriched secreted signalling pathways that altered with aging were the ncWNT pathway, which was enriched in young cells and the growth factor pathways VEGF, IGF, EGF, FGF, and the GAS, PARs, and SPP1 pathways, which were enriched in old cells. ncWNT signalling in young tendon was exerted from FM and IFM tenocytes to FM tenocytes through *WNT11*, and EGF signalling, which was enriched in old tenocytes, was from FM to IFM tenocytes and was through *HBEGF*.

DISCUSSION

This study has unveiled the complexity of cell populations within the tendon IFM for the first time and identified specific populations that are disproportionately affected by aging. The age-related dysregulation of proteostasis and inflammation-related pathways in IFM tenocytes likely has implications for the maintenance of tendon ECM and reparative capacity, respectively, with the potential to influence the risk of tendon injury with aging.

Our results demonstrate that the IFM houses a unique tenocyte population that can be distinguished from fascicular tenocytes due to higher expression of *PRG4* and *TNXB*, and lower expression of *COMP*, *LOX* and *THBS4*. Tendon endothelial, mural and immune cell populations also localise to the IFM, supporting recent work that has identified the presence of an endothelial-like basement membrane in the IFM [45]. Previous scRNAseq studies of mouse and human tendons have identified a range of similar cell populations to those identified in the current study, encompassing tenocytes, endothelial cells and immune cells [12, 13]. While these studies have unveiled

the heterogeneity of tendon cell populations, the majority of murine tendons lack an identifiable IFM. Furthermore, aging processes differ between long-lived and short-lived animals, with continual growth of mice throughout their lifespan, making the mouse an unsuitable model to study the IFM in aging tendon [46, 47]. It is very difficult to collect viable, healthy tendon tissues from young human donors making studies on human tendons impractical. Due to the similarities in tendon pathophysiology between humans and horses and tendon injuries occurring preferentially in elastic tendons with a prominent IFM

such as the equine SDFT, the SDFT is therefore a highly appropriate model in which to study the effect of aging on IFM cell populations. Limitations associated with this model are that the sex, breed and exercise history of the horses are unknown, which may account for the variability between individuals seen in the data, as well as the incomplete annotation of the equine genome. Despite these limitations, we were still able to identify a host of age-related alterations in gene expression between different cell clusters.
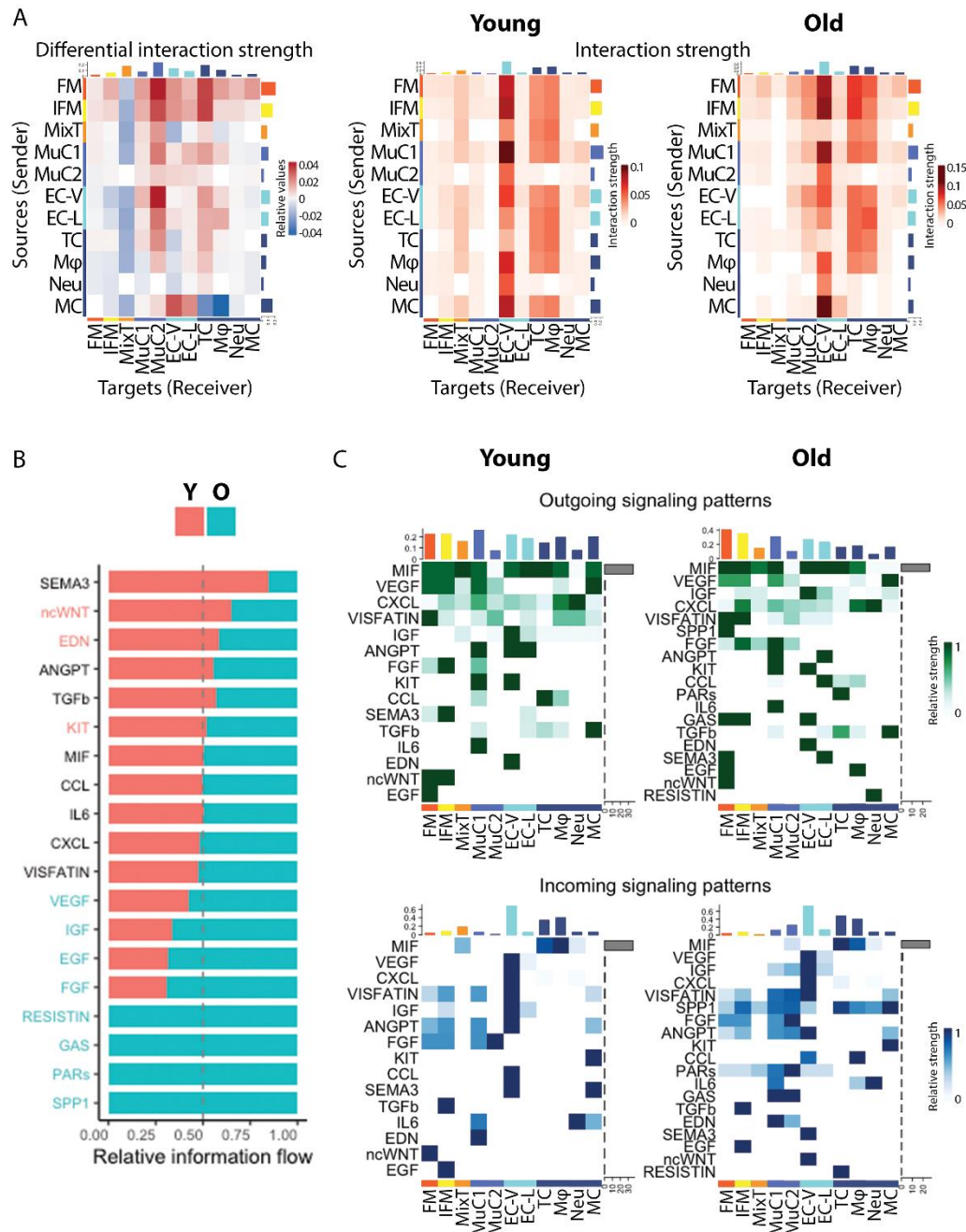
Figure 5. FM and IFM tenocyte clusters become the primary sources of outgoing signalling in aging (n=4/age group). (A) Heatmap of differential secreted signalling interaction strength among tendon clusters following aging, along with the heatmaps of secreted signalling interaction strength among clusters in the young and old tendons. With aging, the FM and IFM tenocyte clusters showed the largest change in outgoing secreted signalling, increasing their signalling interaction strength and becoming the primary sources of outgoing signalling in old tendon cells. Scales indicate relative values and interaction strength and range from blue to red and from white to red, respectively. **(B)** Secreted signalling pathways enriched in young (red) and old (blue) tendon. **(C)** Outgoing and incoming signalling patterns for each secreted signalling pathway and cluster in young and old tendon. Scales indicate relative strength and range from white to green and from white to blue. Significant interactions are identified using a permutation test, p < 0.05.

We identified three tenocyte clusters, two of which were localized to the IFM and FM respectively. The third tenocyte cluster was classed as a mixed tenocyte population (MixT) due to the presence of cells with DE of genes associated with both IFM and FM tenocytes. This clustering was driven by downregulation of ribosomal genes in the mixed tenocytes, which suggests a decreased synthetic activity in these cells [48]. Further analysis of tenocyte subclusters revealed distinct expressions of matrisomal genes, particularly between IFM and FM subclusters, reflecting the differences seen in matrix composition between tendon IFM and FM regions. The low expression of established tenocyte markers *SCX*, *MKX* and *TNMD* in these subclusters is supported by single-cell sequencing data from human and mouse tendons, which also demonstrate limited expression of these markers in adult tenocytes, suggesting that *SCX, MKX* and *TNMD* expressing cells have a more important role in tendon development than in mature tissue [12, 13]. Average *COL1A1* expression was higher in IFM subclusters compared to FM subclusters, which may seem counterintuitive due to the enrichment of type I collagen in the fascicular matrix [8]. However, our previous studies have shown that collagen is turned over more rapidly within the IFM, likely accounting for the increased *COL1A1* gene expression measured within IFM tenocytes [49]. One FM subcluster showed higher expression of mitochondrial-related genes compared to the other tenocyte subclusters. High mitochondrial gene expression has been previously reported in a subset of tenocytes in response to mechanical stimulation and in association with cellular stress [50] and during early healing of tendon in relation to hypoxia in tenocytes [51], but also in dying cells or cells undergoing apoptosis [50]. Here, the FM subcluster showing high mitochondrial gene expression also showed differential expression of genes related to cellular stress but not cell death or apoptosis. As we filtered out dead and dying cells prior to single cell sequencing, we are confident that the high expression of mitochondrial genes in this cluster is not due to cell death induced by sample processing.

The putative tendon progenitor markers *TPPP3* [42] and *POSTN* [43] were also predominantly expressed in the largest IFM subcluster, in particular in a region of the cluster where less differentiated cells were observed, corroborating a less differentiated state for these cells. With aging, *TPPP3* and *POSTN* expression was significantly decreased in IFM tenocytes, as were the number of IFM tenocytes in a less differentiated state, which may provide some insight into the reduced ability for regeneration in aged tendons. Decreased levels of both *TPPP3* and *POSTN* have been reported in other cell types with aging and senescence [52, 53] supporting a putative role for these genes in cell and tissue aging. *TPPP3* expression, however, has also been reported in a tendon immune cell population in mouse tendon [13], indicating these cells may not be true progenitors and as such these markers warrant further investigation in tendon and across species.

One of the key findings of the current study is the age-related alteration of IFM cell populations, with loss of cluster-differentiating gene expression signatures in IFM and MixT tenocyte and mural cell clusters. Similar results have been found in aging skin fibroblasts, with loss of cellular identity and functional priming and reduced cell interactions with increasing age [54]. Aging IFM cell populations also showed dysregulation of senescence-associated genes. Previous studies have demonstrated that human Achilles tendon-derived stem/progenitor cells express several markers of senescence with increasing age [55]. However, no studies have investigated senescence in other tendon cell populations, and this remains an important area for future research. We also identified alterations in a panel of inflammation-associated genes with aging, particularly in IFM tenocytes and mural cells, indicating a deregulated ability to modulate inflammation, which may result in the inflamm-aging phenotype that is seen in aged tendons during injury [56]. A panel of genes associated with loss of proteostasis were also DE with aging. This supports our previous findings, which have demonstrated decreased turnover within the IFM specifically [8]. IFM tenocytes were also the only tenocyte cluster to show age-related changes in cell cycling, with an increase in the percentage of cells in S phase in aged tendons without a concomitant increase in the G2/M phase. Alterations in the duration of the S phase

have been previously noted in senescence and following replicative stress [57, 58] but further investigation is required to elucidate the events leading to the observed increase of cells in S phase and its implications for aged tendon.

Results showed alterations in expression of matrisomal genes with aging in tenocytes, with a general decrease in expression of collagens, with the exception of *COL4A1&2*, which increased in IFM subclusters. These genes encode an integral component of the IFM basement membrane [45], and therefore these changes may result in alterations to IFM basement membrane structure. In addition, the decrease in *LAMA4* expression with aging in tenocytes may have important implications for healing, as it has previously been shown that LAMA4 may be important for the recruitment of IFM cell populations after injury [33]. A decline in the quality of the tendon ECM with aging was also evidenced across IFM and FM regions. Decrease in expression of matrisomal genes, such as *BGN*, *ASPN*, *PRG4*, *FBN1*, *MFAP5* associated with IFM composition and mechanical properties, was noted in IFM tenocytes, whilst *COMP* and *LOX*, associated with FM composition and properties decreased specifically in FM tenocytes [8, 11, 59]. The decline in ECM integrity is considered not only to be fundamental to the functional impairment in tendon but is also a driver of cellular aging and disease progression [60] and as such, of critical importance in aging tendon.

Mural cell aging may also have important implications for tendon function. Few studies have investigated the effect of microvascular cell aging on tendon function, however studies have shown that peritendinous blood flow in the Achilles tendon is lower in aged individuals compared to young individuals [61]. There is also a decrease in the number of capillaries within healthy tendon with aging, and neo-vascularisation is reduced in old rats following injury [62, 63]. These changes may be driven by altered mural cell function due to the dysregulated gene expression described in the current study as well as altered cellular environment. Indeed, age-related microvascular dysfunction is common in other tissues including skeletal muscle [64], with senescence being preceded by vascular attrition in a range of tissues [65]. Pericyte functionality is also diminished with aging, with impaired regenerative capacity in skin [66].

Analysis of cell-to-cell communication predicted a complex signalling network between tendon cell populations that was altered with aging, particularly in tenocytes, mural cells, and T cells. This alone highlights the importance of elucidating the heterogeneity of tendon cell populations and the importance of using co-culture systems to recapitulate complex in vivo interactions. Of note, SPP1 and EGF signalling through *HBEGF*, which

have been reported to participate in the active remodelling of tendon during injury repair [67], were enriched in aged tendons.

The discovery of the extensive heterogeneity of tendon cell populations has important implications for studying tendon-derived cells *in vitro*. The response of tendon-derived cells to a wide variety of physicochemical stimuli has been extensively characterised *in vitro* [68, 69], however, these studies have typically assumed that tendon-derived cells are a homogenous population of fibroblastic-like tenocytes, utilising culture conditions and experimental conditions appropriate for such a population, potentially impacting the relevance of such results to *in vivo* tendon cell behaviour. Identification of markers for each tendon cell population will allow future studies to use cell sorting approaches to study responses of individual populations in isolation or in specific combinations, which will provide much more in-depth information on the role of each population in tendon homeostasis, aging and injury. However, it will be important to optimise culture conditions to ensure phenotypic stability is maintained in these different cell populations.

While this study has identified novel IFM-localised cell populations that are prone to age-related dysfunction, there is a pressing need to define the mechanisms that are driving these age-related alterations. Previous studies have demonstrated that the IFM is disproportionately affecting by aging, with stiffening occurring, likely due to accumulation of microdamage and reduced protein turnover [8, 11, 19]. These changes will likely alter the cell microenvironment, which could negatively affect cell phenotype and lead to the age-related changes observed in the current study. Additionally, the accumulation of non-enzymatic modifications within extracellular matrix proteins, which are common in aging tendon, have been found to induce cell senescence and tissue fibrosis [70-72]. Alternatively, there may be intrinsic changes within IFM cell populations driving age-related alterations in cell phenotype. This remains an important area for future research to allow development of therapeutics that can effectively limit and/or reverse tendon age-related dysfunction and subsequent injury.

We have uncovered the heterogeneity of IFM-localised cell populations within tendon, revealing the presence of diverse cell types including tenocytes, microvascular cells and immune cells. The IFM cell populations are disproportionately affected by aging, with dysregulation of genes associated with senescence, proteostasis and inflammation, making these cells likely targets when developing more effective therapeutics for age-related tendon injury.

Disclosure Statement

The authors have no conflicts of interest to declare.

Supplementary Materials

The Supplementary data can be found online at: www.aginganddisease.org/EN/10.14336/AD.2023.0425-1.

References

[1]   Clayton RAE, Court-Brown CM (2008). The epidemiology of musculoskeletal tendinous and ligamentous injuries. Injury, 39:1338-1344.

[2]   Perkins NR, Reid SWJ, Morris RS (2005). Risk factors for injury to the superficial digital flexor tendon and suspensory apparatus in Thoroughbred racehorses in New Zealand. N Z Vet J, 53:184 - 192.

[3]   Biewener AA (1998). Muscle-tendon stresses and elastic energy storage during locomotion in the horse. Comparative Biochemistry and Physiology Part B: Biochemistry and Molecular Biology, 120:73-87.

[4]   Lichtwark GA, Wilson AM (2007). Is Achilles tendon compliance optimised for maximum muscle efficiency during locomotion? J Biomech, 40:1768-1775.

[5]   Patterson-Kane JC, Rich T (2014). Achilles tendon injuries in elite athletes: lessons in pathophysiology from their equine counterparts. Ilar j, 55:86-99.

[6]   Innes JF, Clegg P (2010). Comparative rheumatology: what can be learnt from naturally occurring musculoskeletal disorders in domestic animals? Rheumatol (Oxford), 49:1030-1039.

[7]   Kastelic J, Galeski A, Baer E (1978). The multicomposite structure of tendon. Connect Tissue Res, 6:11-23.

[8]   Thorpe CT, Peffers MJ, Simpson D, Halliwell E, Screen HR, Clegg PD (2016). Anatomical heterogeneity of tendon: Fascicular and interfascicular tendon compartments have distinct proteomic composition. Scientific Reports, 6:20455.

[9]   Thorpe CT, Karunaseelan KJ, Ng Chieng Hin J, Riley GP, Birch HL, Clegg PD, et al. (2016). Distribution of proteins within different compartments of tendon varies according to tendon type. Journal of Anatomy, 229:450-458.

[10]   Godinho MS, Thorpe CT, Greenwald SE, Screen HRC (2021). Elastase treatment of tendon specifically impacts the mechanical properties of the interfascicular matrix. Acta biomaterialia, 123:187-196.

[11]   Godinho MSC, Thorpe CT, Greenwald SE, Screen HRC (2017). Elastin is Localised to the Interfascicular Matrix of Energy Storing Tendons and Becomes Increasingly Disorganised With Ageing. Scientific Reports, 7:9713.

[12]   Kendal AR, Layton T, Al-Mossawi H, Appleton L, Dakin S, Brown R, et al. (2020). Multi-omic single cell analysis resolves novel stromal cell populations in healthy and diseased human tendon. Scientific Reports, 10:13939.

[13]   De Micheli AJ, Swanson JB, Disser NP, Martinez LM, Walker NR, Oliver DJ, et al. (2020). Single-cell transcriptomic analysis identifies extensive heterogeneity in the cellular composition of mouse Achilles tendons. American Journal of Physiology-Cell Physiology, 319:C885-C894.

[14]   Obuchowicz R, Ekiert M, Kohut P, Holak K, Ambrozinski L, Tomaszewski KA, et al. (2019). Interfascicular matrix-mediated transverse deformation and sliding of discontinuous tendon subcomponents control the viscoelasticity and failure of tendons. Journal of the Mechanical Behavior of Biomedical Materials, 97:238-246.

[15]   Thorpe CT, Udeze CP, Birch HL, Clegg PD, Screen HR (2012). Specialization of tendon mechanical properties results from interfascicular differences. J R Soc Interface, 9:3108-3117.

[16]   Thorpe CT, Godinho MS, Riley GP, Birch HL, Clegg PD, Screen HR (2015). The interfascicular matrix enables fascicle sliding and recovery in tendon, and behaves more elastically in energy storing tendons. Journal of the Mechanical Behavior of Biomedical Materials, 52:85-94.

[17]   Thorpe CT, Riley GP, Birch HL, Clegg PD, Screen HR (2016). Fascicles and the interfascicular matrix show adaptation for fatigue resistance in energy storing tendons. Acta Biomater, 42:308-315.

[18]   Mlyniec A, Dabrowska S, Heljak M, Weglarz WP, Wojcik K, Ekiert-Radecka M, et al. (2021). The dispersion of viscoelastic properties of fascicle bundles within the tendon results from the presence of interfascicular matrix and flow of body fluids. Mater Sci Eng C Mater Biol Appl, 130:112435.

[19]   Thorpe CT, Udeze CP, Birch HL, Clegg PD, Screen HR (2013). Capacity for sliding between tendon fascicles decreases with ageing in injury prone equine tendons: a possible mechanism for age-related tendinopathy? Eur Cell Mater, 25:48-60.

[20]   Thorpe CT, Riley GP, Birch HL, Clegg PD, Screen HRC (2017). Fascicles and the interfascicular matrix show decreased fatigue life with ageing in energy storing tendons. Acta Biomater, 56:58-64.

[21]   Patel D, Zamboulis DE, Spiesz EM, Birch HL, Clegg PD, Thorpe CT, et al. (2021). Structure-function specialisation of the interfascicular matrix in the human

achilles tendon. Acta Biomaterialia.

[22] Griffiths JA, Richard AC, Bach K, Lun ATL, Marioni JC (2018). Detection and removal of barcode swapping in single-cell RNA-seq data. Nature Communications, 9:2667.

[23] Butler A, Hoffman P, Smibert P, Papalexi E, Satija R (2018). Integrating single-cell transcriptomic data across different conditions, technologies, and species. Nature Biotechnology, 36:411-420.

[24] Hafemeister C, Satija R (2019). Normalization and variance stabilization of single-cell RNA-seq data using regularized negative binomial regression. Genome Biology, 20:296.

[25] Korsunsky I, Millard N, Fan J, Slowikowski K, Zhang F, Wei K, et al. (2019). Fast, sensitive and accurate integration of single-cell data with Harmony. Nature Methods, 16:1289-1296.

[26] Consortium AA (2020). Aging Atlas: a multi-omics database for aging biology. Nucleic Acids Research, 49:D825-D830.

[27] Smith CL, Eppig JT (2009). The mammalian phenotype ontology: enabling robust annotation and comparative analysis. Wiley Interdiscip Rev Syst Biol Med, 1:390-399.

[28] Shao X, Taha IN, Clauser KR, Gao Y, Naba A (2019). MatrisomeDB: the ECM-protein knowledge database. Nucleic Acids Research, 48:D1136-D1144.

[29] Gu Z, Gu L, Eils R, Schlesner M, Brors B (2014). circlize Implements and enhances circular visualization in R. Bioinformatics, 30:2811-2812.

[30] Gulati GS, Sikandar SS, Wesche DJ, Manjunath A, Bharadwaj A, Berger MJ, et al. (2020). Single-cell transcriptional diversity is a hallmark of developmental potential. Science, 367:405-411.

[31] Allen M, Poggiali D, Whitaker K, Marshall T, van Langen J, Kievit R (2021). Raincloud plots: a multi-platform tool for robust data visualization [version 2; peer review: 2 approved]. Wellcome Open Research, 4.

[32] Jin S, Guerrero-Juarez CF, Zhang L, Chang I, Ramos R, Kuan C-H, et al. (2021). Inference and analysis of cell-cell communication using CellChat. Nature Communications, 12:1088.

[33] Marr N, Meeson R, Kelly EF, Fang Y, Peffers MJ, Pitsillides AA, et al. (2021). CD146 Delineates an Interfascicular Cell Sub-Population in Tendon That Is Recruited during Injury through Its Ligand Laminin-α4. Int J Mol Sci, 22.

[34] Södersten F, Hultenby K, Heinegård D, Johnston C, Ekman S (2013). Immunolocalization of Collagens (I and III) and Cartilage Oligomeric Matrix Protein in the Normal and Injured Equine Superficial Digital Flexor Tendon. Connective Tissue Research, 54:62-69.

[35] Frolova EG, Drazba J, Krukovets I, Kostenko V, Blech L, Harry C, et al. (2014). Control of organization and function of muscle and tendon by thrombospondin-4. Matrix Biol, 37:35-48.

[36] Sun Y-L, Wei Z, Zhao C, Jay GD, Schmid TM, Amadio PC, et al. (2015). Lubricin in human achilles tendon: The evidence of intratendinous sliding motion and shear force in achilles tendon. Journal of Orthopaedic Research, 33:932-937.

[37] Vanlandewijck M, He L, Mäe MA, Andrae J, Ando K, Del Gaudio F, et al. (2018). A molecular atlas of cell types and zonation in the brain vasculature. Nature, 554:475-480.

[38] Muhl L, Genové G, Leptidis S, Liu J, He L, Mocci G, et al. (2020). Single-cell analysis uncovers fibroblast heterogeneity and criteria for fibroblast and mural cell identification and discrimination. Nature Communications, 11:3953.

[39] Gross SR, Sin CGT, Barraclough R, Rudland PS (2014). Joining S100 proteins and migration: for better or for worse, in sickness and in health. Cellular and Molecular Life Sciences, 71:1551-1579.

[40] Cerezo LA, Remáková M, Tomčik M, Gay S, Neidhart M, Lukanidin E, et al. (2014). The metastasis-associated protein S100A4 promotes the inflammatory response of mononuclear cells via the TLR4 signalling pathway in rheumatoid arthritis. Rheumatology (Oxford), 53:1520-1526.

[41] Turlo AJ, Mueller-Breckenridge AJ, Zamboulis DE, Tew SR, Canty-Laird EG, Clegg PD (2019). Insulin-like growth factor binding protein (IGFBP6) is a cross-species tendon marker. Eur Cell Mater, 38:123-136.

[42] Harvey T, Flamenco S, Fan CM (2019). A Tppp3(+)Pdgfra(+) tendon stem cell population contributes to regeneration and reveals a shared role for PDGF signalling in regeneration and fibrosis. Nat Cell Biol, 21:1490-1503.

[43] Wang Y, Jin S, Luo D, He D, Shi C, Zhu L, et al. (2021). Functional regeneration and repair of tendons using biomimetic scaffolds loaded with recombinant periostin. Nat Commun, 12:1293.

[44] Mori N, Majima T, Iwasaki N, Kon S, Miyakawa K, Kimura C, et al. (2007). The role of osteopontin in tendon tissue remodeling after denervation-induced mechanical stress deprivation. Matrix Biol, 26:42-53.

[45] Marr N, Zamboulis DE, Werling D, Felder AA, Dudhia J, Pitsillides AA, et al. (2022). The tendon interfascicular basement membrane provides a vascular niche for CD146+ pericyte cell subpopulations. Front Cell Dev Biol.

[46] Jilka RL (2013). The relevance of mouse models for investigating age-related bone loss in humans. The journals of gerontology. Series A, Biological sciences and medical sciences, 68:1209-1217.

[47] Lee AH, Elliott DM (2019). Comparative multi-scale hierarchical structure of the tail, plantaris, and Achilles tendons in the rat. J Anat, 234:252-262.

[48] Steffen KK, Dillin A (2016). A Ribosomal Perspective on Proteostasis and Aging. Cell Metabolism, 23:1004-1012.

[49] Choi H, Simpson D, Wang D, Prescott M, Pitsillides AA, Dudhia J, et al. (2020). Heterogeneity of proteome dynamics between connective tissue phases of adult tendon. eLife, 9:e55262.

[50] Still C, II, Chang W-T, Sherman SL, Sochacki KR, Dragoo JL, Qi LS (2021). Single-cell transcriptomic profiling reveals distinct mechanical responses between normal and diseased tendon progenitor cells. Cell Reports Medicine, 2.

[51] Thankam FG, Chandra IS, Kovilam AN, Diaz CG, Volberding BT, Dilisio MF, et al. (2018). Amplification of Mitochondrial Activity in the Healing Response Following Rotator Cuff Tendon Injury. Sci Rep, 8:17027.

[52] Egbert M, Ruetze M, Sattler M, Wenck H, Gallinat S, Lucius R, et al. (2014). The matricellular protein periostin contributes to proper collagen function and is downregulated during skin aging. Journal of Dermatological Science, 73:40-48.

[53] Schwartz RE, Shokhirev MN, Andrade LR, Gutkind JS, Iglesias-Bartolome R, Shadel GS (2021). Insights into epithelial cell senescence from transcriptome and secretome analysis of human oral keratinocytes. Aging (Albany NY), 13:4747-4777.

[54] Solé-Boldo L, Raddatz G, Schütz S, Mallm JP, Rippe K, Lonsdorf AS, et al. (2020). Single-cell transcriptomes of the human skin reveal age-related loss of fibroblast priming. Commun Biol, 3:188.

[55] Kohler J, Popov C, Klotz B, Alberton P, Prall WC, Haasters F, et al. (2013). Uncovering the cellular and molecular changes in tendon stem/progenitor cells attributed to tendon aging and degeneration. Aging Cell, 12:988-999.

[56] Dakin SG, Dudhia J, Werling NJ, Werling D, Abayasekara DRE, Smith RKW (2012). Inflamm-Aging and Arachadonic Acid Metabolite Differences with Stage of Tendon Disease. PLoS ONE, 7:e48978.

[57] Prieur A, Besnard E, Babled A, Lemaitre JM (2011). p53 and p16(INK4A) independent induction of senescence by chromatin-dependent alteration of S-phase progression. Nat Commun, 2:473.

[58] Ercilla A, Llopis A, Feu S, Aranda S, Ernfors P, Freire R, et al. (2016). New origin firing is inhibited by APC/CCdh1 activation in S-phase after severe replication stress. Nucleic Acids Res, 44:4745-4762.

[59] Zamboulis DE, Thorpe CT, Ashraf Kharaz Y, Birch HL, Screen HRC, Clegg PD (2020). Postnatal mechanical loading drives adaptation of tissues primarily through modulation of the non-collagenous matrix. eLife, 9:e58075.

[60] Ewald CY (2020). The Matrisome during Aging and Longevity: A Systems-Level Approach toward Defining Matreotypes Promoting Healthy Aging. Gerontology, 66:266-274.

[61] Langberg H, Olesen J, Skovgaard D, Kjær M (2001). Age related blood flow around the Achilles tendon during exercise in humans. European Journal of Applied Physiology, 84:246-248.

[62] Kannus P, Paavola M, Józsa L. 2005. Aging and Degeneration of Tendons. In Tendon Injuries: Basic Science and Clinical Medicine. N. Maffulli, P. Renström, and W.B. Leadbetter, editors. London: Springer London. 25-31.

[63] Riggin CN, Weiss SN, Rodriguez AB, Raja H, Chen M, Schultz SM, et al. (2022). Increasing Vascular Response to Injury Improves Tendon Early Healing Outcome in Aged Rats. Annals of Biomedical Engineering, 50:587-600.

[64] Scioli MG, Bielli A, Arcuri G, Ferlosio A, Orlandi A (2014). Ageing and microvasculature. Vascular Cell, 6:19.

[65] Chen J, Sivan U, Tan SL, Lippo L, De Angelis J, Labella R, et al. (2021). High-resolution 3D imaging uncovers organ-specific vascular control of tissue aging. Science Advances, 7:eabd7819.

[66] Zhuang L, Visalakshan RM, Kaur P (2021). Dermal Pericytes Exhibit Declined Ability to Promote Human Skin Regeneration with Ageing in 3D Organotypic Culture Models. Cells, 10.

[67] Ackerman JE, Best KT, Muscat SN, Wu C-L, Loiselle AE (2021). Defining the activation profile and fate trajectory of adult Scleraxis-lineage cells during tendon healing by combining lineage tracing and spatial transcriptomics. bioRxiv:2021.2006.2002.446663.

[68] Wall ME, Dyment NA, Bodle J, Volmer J, Loboa E, Cederlund A, et al. (2016). Cell Signaling in Tenocytes: Response to Load and Ligands in Health and Disease. Adv Exp Med Biol, 920:79-95.

[69] Ryan CNM, Pugliese E, Shologu N, Gaspar D, Rooney P, Islam MN, et al. (2021). A combined physicochemical approach towards human tenocyte phenotype maintenance. Mater Today Bio, 12:100130.

[70] Fedintsev A, Moskalev A (2020). Stochastic non-enzymatic modification of long-lived macromolecules - A missing hallmark of aging. Ageing Res Rev, 62:101097.

[71] Thorpe CT, Streeter I, Pinchbeck GL, Goodship AE, Clegg PD, Birch HL (2010). Aspartic acid racemization and collagen degradation markers reveal an accumulation of damage in tendon collagen that is enhanced with aging. Journal of Biological Chemistry, 285:15674-15681.

[72] Selman M, Pardo A (2021). Fibroageing: An ageing pathological feature driven by dysregulated extracellular matrix-cell mechanobiology. Ageing Research Reviews, 70:101393.